Journal of Materials Chemistry B

Materials for biology and medicine

www.rsc.org/MaterialsB

Volume 1 | Number 34 | 14 September 2013 | Pages 4191–4350

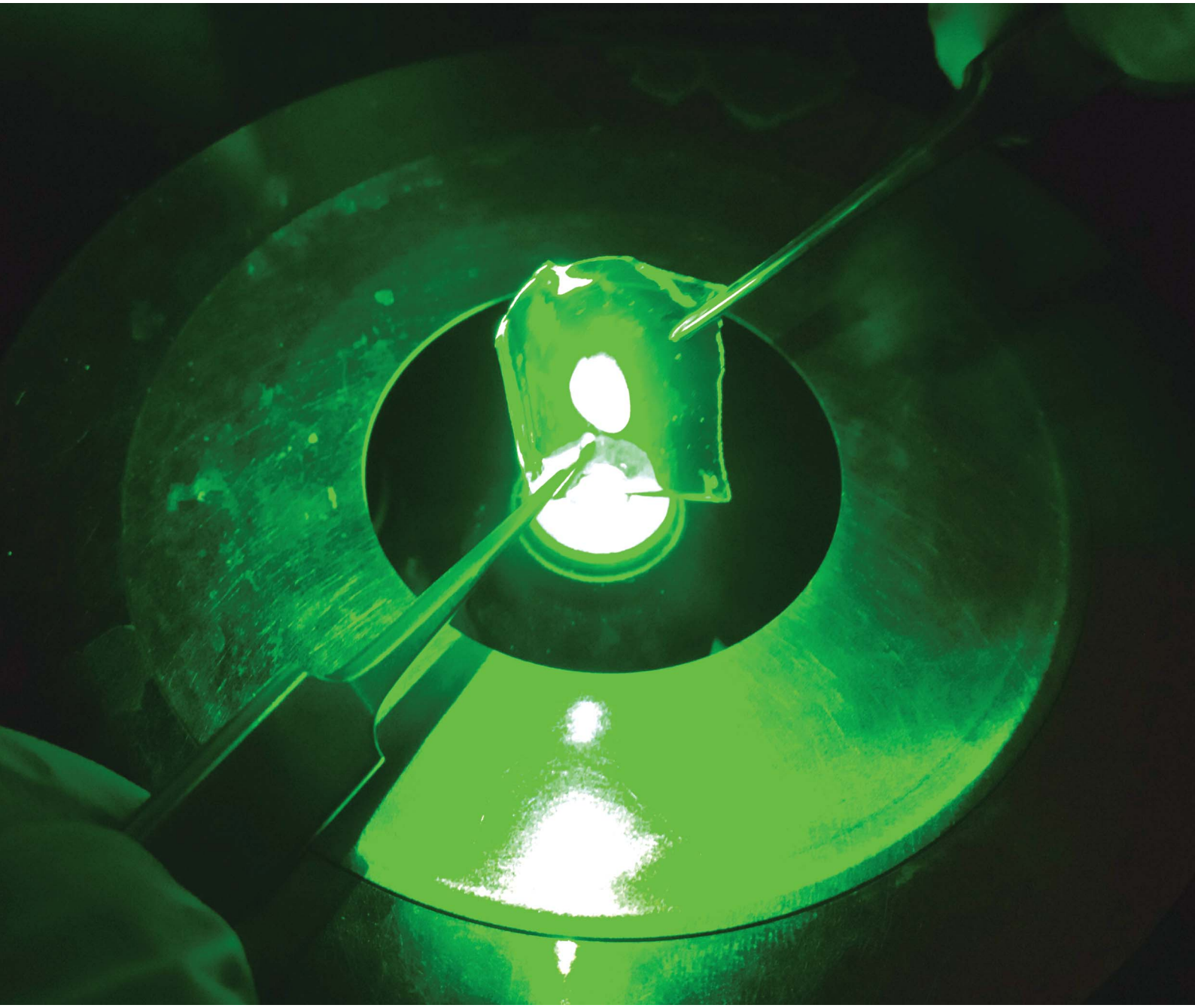

ISSN 2050-750X

RSC Publishing

PAPER

Ali Khademhosseini, Marco Rolandi *et al.*

Chitin nanofiber micropatterned flexible substrates for tissue engineering

2050-750X(2013)1:34;1-S

Journal of Materials Chemistry B

RSC Publishing

PAPER

View Article Online
View Journal | View Issue

Chitin nanofiber micropatterned flexible substrates for tissue engineering†

Cite this: *J. Mater. Chem. B*, 2013, **1**, 4217

Pegah Hassanzadeh,‡[a] Mahshid Kharaziha,‡[bc] Mehdi Nikkhah,[bc] Su Ryon Shin,[bcd] Jungho Jin,[a] Simeiqi He,[a] Wei Sun,[a] Chao Zhong,[a] Mehmet R. Dokmeci,[bcd] Ali Khademhosseini*[bcd] and Marco Rolandi*[a]

Engineered tissues require enhanced organization of cells and the extracellular matrix (ECM) for proper function. To promote cell organization, substrates with controlled micro- and nanopatterns have been developed as supports for cell growth, and to induce cellular elongation and orientation *via* contact guidance. Micropatterned ultra-thin biodegradable substrates are desirable for implantation in the host tissue. These substrates, however, need to be mechanically robust to provide substantial support for the generation of new tissues, to be easily retrievable, and to maintain proper handling characteristics. Here, we introduce ultra-thin (<10 μm), self-assembled chitin nanofiber substrates micropatterned by replica molding for engineering cell sheets. These substrates are biodegradable, mechanically strong, yet flexible, and can be easily manipulated into the desired shape. As a proof-of-concept, fibroblast cell attachment, proliferation, elongation, and alignment were studied on the developed substrates with different pattern dimensions. On the optimized substrates, the majority of the cells aligned (<10°) along the major axis of micropatterned features. With the ease of fabrication and mechanical robustness, the substrates presented herein can be utilized as a versatile system for the engineering and delivery of ordered tissue in applications such as myocardial repair.

Received 3rd June 2013
Accepted 8th July 2013

DOI: 10.1039/c3tb20782j

www.rsc.org/MaterialsB

Introduction

Engineered tissues require enhanced organization of cells and the extracellular matrix (ECM) for proper function.[1–3] The cells reorganize according to the interaction with the ECM based on topography and mechanical properties such as matrix stiffness, elasticity, and viscosity.[4] Alignment of ECM molecules and concentration gradients of immobilized growth factors also play a crucial role in cellular organization.[3] To promote cellular organization, substrates with controlled micro- and nanopatterns have been developed as supports for cell growth, and to induce cellular elongation and orientation *via* contact guidance in engineered tissues.[5–11] These substrates produce highly ordered and functional cell-sheets that may be detached from the substrate for delivery to the host tissue *via* enzymatic degradation or thermal stimulus.[12–17] Delivery of the engineered cell-sheets often occurs with a support platform because free-standing cell sheets are mechanically weak and difficult to handle.[18] An alternate approach is to create cell-sheets on ultra-thin biodegradable substrates that are implanted in the host tissue. These substrates need to be thin and flexible for conformal contact to the tissue of choice and robust for the ease of handling.[19] Robustness of the substrate is particularly important in myocardial tissue repair.[16,17] During this repair, the cell carrying substrate is also required to restore the mechanical properties of the damaged tissue while the new tissue is growing. To fabricate robust biodegradable substrates, structural biopolymers such as collagen, chitin, and chitosan are particularly appealing for their biocompatibility and mechanical strength.[20–22] Specifically, chitin and its deacetylated derivative, chitosan, possess multiple advantages as tissue engineering substrates including nontoxicity, cytocompatibility, and tunable biodegradability.[20,23–28] In addition, the 3-D assembly of nanofibrous structures with chitin and chitosan is known to mimic the natural ECM and promote cell attachment and spreading ability.[29] While chitin nanofibers already exist in nature, chitosan nanofibers are typically produced by electrospinning.[30–32] Electrospinning is difficult to couple with micro- and nanofabrication to yield micropatterned substrates. However, chitosan nanofibers have found broader use than

[a]*Department of Materials Science and Engineering, University of Washington, Seattle, WA, 98195, USA. E-mail: rolandi@uw.edu*

[b]*Center for Biomedical Engineering, Department of Medicine, Brigham and Women's Hospital, Harvard Medical School, Boston, MA 02115, USA. E-mail: alik@rics.bwh.harvard.edu*

[c]*Harvard-MIT Division of Health Sciences and Technology, Massachusetts Institute of Technology, Cambridge, MA 02139, USA*

[d]*Wyss Institute for Biologically Inspired Engineering, Harvard University, Boston, MA 02115, USA*

† Electronic supplementary information (ESI) available. See DOI: 10.1039/c3tb20782j

‡ These authors contributed equally to this work.

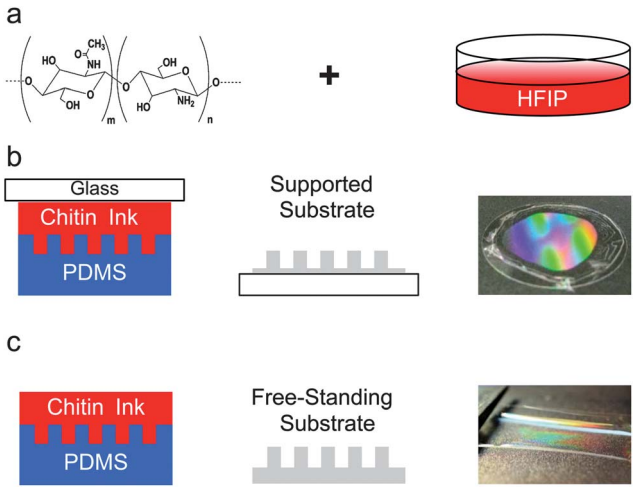

Fig. 1 Chitin nanofiber-based micropatterned substrate fabrication process. (a) Chitin/HFIP solution (0.1% w/w) was poured on top of the (b) mold covered with a glass slide to create a supported substrate after drying overnight and substrate optical image with the diffraction pattern. (c) Thicker films were obtained from more concentrated solutions (0.2% w/w) to create free-standing substrates, which were robust and easy to handle. The optical image demonstrated the diffraction pattern on the free-standing chitin film.

chitin due to chitin's intractability and insolubility in common organic solvents. We have previously demonstrated the self-assembly of ultrathin (3 nm) α-chitin nanofibers from solution[33] and the micro- and nanofabrication of self-assembled chitin nanofiber structures with soft lithography strategies.[34] Here, we utilize this facile and versatile approach to produce transparent, ultra-thin (<10 μm), mechanically robust, yet flexible self-assembled chitin nanofiber micropatterned substrates for tissue engineering (Fig. 1). With these micropatterned substrates, we demonstrated cell sheets of aligned fibroblasts as a proof of concept. The supported cell sheets made in this manner were mechanically robust and easy to handle, yet flexible and bendable in the shape of choice.

Experimental

Fabrication of chitin substrates

Substrates with micropatterns were fabricated using replica molding from a "chitin nanofiber ink" as previously described.[34] The chitin nanofiber ink was prepared by stirring an appropriate amount of β-chitin squid extract (Industrial Research Ltd-New Zealand) in hexafluoro-2-propanol (HFIP) (Oakwood Products, Inc.) for one week under ambient conditions. The starting material had a degree of acetylation defined as $n/(m+n)$ (Fig. 1a) of 84%. Two optical gratings (THORLABS) were used as masters: GE2550-3263 Echelle Grating with 3.16 μm spacing and 63° blaze angle (G1) and a GE 2550-0875 Echelle Grating, 12.66 μm, 75° blaze angle (G2). Replica molds were made with polydimethylsiloxane (PDMS) from SYLGARD 184 (10% curing agent) and cured at 50 °C for 8 hours. The chitin nanofiber ink was drop cast onto the mold (50 μl) to create the micropatterned features. Alternatively, control substrates (no micropatterns) were prepared using a flat PDMS mold. The micropatterned and control substrates were supported on plasma-cleaned glass cover slips (Ted Pella, Inc.). For supported micropatterned and control substrates, a chitin solution of 0.1% w/w was used. Free-standing chitin substrates were fabricated with a 0.2% w/w chitin solution. Solutions of higher concentrations resulted in thicker films that were easier to handle. Both types of films were dried overnight under ambient conditions and peeled off from the PDMS mold for further experiments.

Characterization of chitin substrates

A Veeco Multimode V (Nanoscope IV controller) and Veecoprobes Sb-doped Si cantilevers ($\rho = 0.01$–$0.025\ \Omega$ cm, $k = 40$ N m^{-1}, $\upsilon \sim 300$ kHz) were used for atomic force microscopy (AFM). Fourier transform infrared (FTIR) spectra were recorded on free-standing substrates using a Bruker vector 33 FTIR spectrophotometer (4000 to 400 cm^{-1}, 4 cm^{-1} resolution). The degree of deacetylation (chitin *vs.* chitosan) was evaluated using the ratio of A_{1560}/A_{1030} according to a previously reported procedure.[28,35] Stress *vs.* strain data of the free-standing substrates were recorded with a Shimadzu AGS-X. The substrates were tested dry before and after deacetylation as well as after immersion in Dulbecco's Phosphate Buffered Saline (DPBS) (GIBCO) for 1 and 5 days. Wet substrates were immersed in DPBS for 1 day and tested immediately after removing from the solution.

Chemical modification of chitin substrates

Chitin substrates were partially deacetylated and coated with fibronectin (FN) to improve cell attachment and proliferation. Deacetylation was performed with 5 mM NaOH at 40 °C for 1 hour. The substrates were then washed with distilled water three times and air-dried. FN (from bovine plasma, 0.1% sterile solution, Sigma-Aldrich) was coated on the substrate by incubating the chitin substrates in 200 μl of FN solution (50 μl ml^{-1}… in DPBS) for two hours ($T = 37$ °C). After incubation, the substrates were rinsed thoroughly in DPBS to remove the non-adsorbed and excessive aggregates of FN. The substrates were then dried in a desiccator overnight for further biological experiments.

Cell culture preparation

NIH-3T3 fibroblast cells were used in this work. The cells were maintained in T-75 flasks at 37 °C and 5% CO_2 and cultured in Dulbecco's Modified Eagle Medium (DMEM) supplemented with 10% FBS and 1% penicillin–streptomycin. Prior to seeding cells on chitin substrates, the samples were rinsed in NIH-3T3 cell culture medium twice. 80% confluent 3T3 cells were trypsinized, washed and suspended in fresh culture medium and subsequently the cell suspension was diluted with cell growth medium to reach the desired cell concentration. A cell suspension containing 1000 cells per 500 μl of medium was then added to each sample for further testing.

Cell proliferation and immunofluorescence for cytoskeletal organization

Cell attachment and proliferation on the micropatterned and control (without pattern) chitin substrates were evaluated by

direct cell counting at days 0 and 5 of culture. Immunostaining assesses the actin cytoskeletal organization (F-actin) of the cells attached to different samples. The samples were washed three times in DPBS and were fixed in 4% paraformaldehyde (PF) solution in DPBS for 20 min at room temperature. The substrates were then submerged in 0.1% Triton X-100 solution in DPBS for 30 minutes in order to permeabilize the cell membranes and blocked in 1% bovine serum albumin (BSA) for 1 h. The actin cytoskeleton was stained using 1 : 40 dilution of Alexa Fluor-594 phalloidin (Invitrogen) in 1% BSA. Following immunostaining, the cell nuclei were stained with 1 : 1000 dilution of 4′,6-diamidino-2-phenyl indole dihydrochloride (DAPI) stain (Invitrogen) in DPBS for 5 min. Upon staining, the samples were imaged using an inverted fluorescence microscope (Nikon TE 2000-U, Nikon instruments Inc., USA) and the fluorescence images were analyzed using NIH Image J software (version 1.4).

Quantification of cellular alignment and shape index

To quantify cellular alignment on micropatterned and control chitin substrates, fluorescence images were obtained at 5–6 different locations of each sample after 5 days of culture. The shape of each individual nucleus was first fitted with an ellipse and the normalized nuclei alignment was defined according to a previously published procedure.[36] The normalized cellular alignment angles were finally grouped in 10 degree increments to compare the alignment of nuclei on patterned and control substrates. Cell elongation within each sample was evaluated using fluorescence images of the cells' cytoskeleton stained for F-actin filaments (5–6 regions). Cell elongation was determined as the ratio of cell length to cell width. The cell length was defined as its longest chord and the cell width was defined as the longest chord perpendicular to its length. The angle between the cells longest chord and the direction of the micropattern grating was defined as the cell orientation angle.

Results and discussion

We prepared the chitin micropatterned substrates by replica molding of a "chitin nanofiber ink" (Fig. 1). The chitin nanofiber ink is a solution of squid pen β-chitin that self-assembles into 3 nm diameter α-chitin nanofibers upon drying.[33,34] To create the desired substrates, an appropriate amount of chitin nanofiber ink was drop cast on top of the mold and allowed to dry overnight under ambient conditions. In this work, we used PDMS replica of different gratings as molds to create the substrates. We chose micropatterns with 3.16 μm spacing (G1) and 12 μm spacing (G2) to evaluate the effects of groove spacing on cell alignment, G1 being smaller than the average cell diameter, and G2 being slightly larger than the average cell diameter. Supported chitin micropatterned substrates were

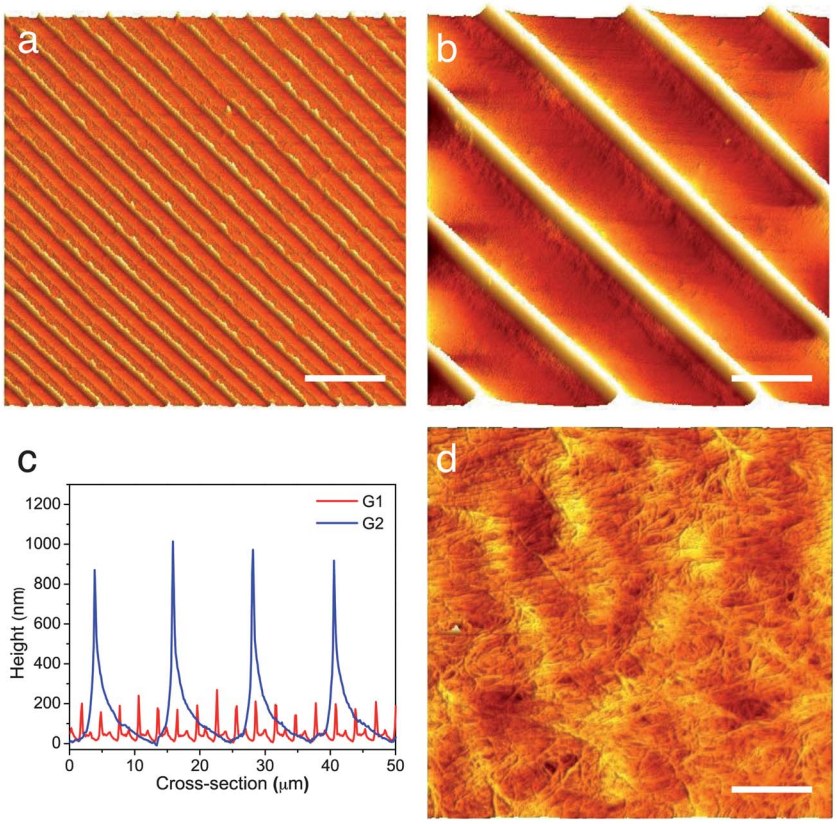

Fig. 2 AFM imaging of the supported chitin substrates. (a and b) AFM height images of chitin substrates G1 and G2, respectively (scale bar: 10 μm). (c) Cross-sectional height profiles of (a) and (b). G1 pitch = 3.0 ± 0.09 μm and height = 193.4 ± 30.4 nm and G2 pitch = 12.2 ± 0.2 μm and height 943.3 ± 62.6 nm. (d) Magnified view of (b) showing the chitin nanofiber morphology (scale bar = 200 nm).

obtained by placing a glass slide on the top of the solution during drying (Fig. 1b). This simple strategy afforded the attachment of chitin nanofiber substrates to an arbitrary support without requiring additional adhesives, which may be toxic for the cells. Free-standing substrates were typically thicker than the supported substrates and were peeled off directly from the mold (Fig. 1c). The free-standing substrates were robust and could be easily lifted out from the molds with a pair of lab-tweezers. Both supported and free-standing substrates were easy to handle and stable in cell culture media for extended periods of time. The microfabricated substrates prepared in this fashion exhibited the desired microstructure, which is inferred from the diffraction patterns in the optical images (Fig. 1b and c) and AFM micrographs (Fig. 2a and b). Micropatterned substrates G1 and G2 closely replicated the spacing and height of the original gratings (Fig. 2c). Both G1 and G2 substrates had a saw tooth cross-section that derived from the cross-section of the diffraction grating. The features in G1 were on average 193 nm tall, while the features on the G2 substrates were 943 nm tall. For both substrates, uniform features were found in extended areas of up to several cm^2 only limited by the size of the original master and mold. With appropriate masters and molds, features of arbitrary shape and size ranging from a few nanometers to hundreds of microns were also available with the "chitin nanofiber ink" expanding the kind of substrates available for future studies. Over fifty substrates were reliably reproduced from the same master without observing any degradation of the replicated master. Each PDMS mold was reused at most ten times before noticing some degradation of the patterns due to mold contamination with the chitin material. As previously reported, the random morphology of chitin nanofibers was maintained intact in the micropatterns with the replica molding process (Fig. 2d).[34] In the future, substrates with chitin nanofibers aligned along the micropattern direction may be fabricated with directional drying.[33] This replica molding process was low cost, easy to use, high throughput, and did not require expensive clean room equipment. With this simple solution processing micropatterned supported and free-standing substrates were created in one step for further experiments.

To employ the micropatterned nanofiber substrates for tissue engineering, NIH-3T3 fibroblast cells were seeded on the substrates with different sizes of grooves and their behavior was subsequently investigated. We chose fibroblasts for proof-of-concept because the organization of fibroblasts within the ECM of native myocardial tissue is critical to cell alignment, which influences the electrical and mechanical properties of the heart.[37] Fibroblast cell attachment to the as-prepared chitin substrates was low, as previously observed for neuronal cells, possibly due to the lack of reactive species and positive charges on the chitin surface.[28] To improve cell attachment, the chitin substrates were partially deacetylated and coated with a thin layer of FN. FN is an ECM protein and plays a major role in cell adhesion, growth, migration, and differentiation.[38] Deacetylation replaced the acetyl group in chitin (Fig. 1a, *n* block) with an amine (Fig. 1a, *m* block) resulting in a more hydrophilic and positively charged polymer. When the ratio between acetyl groups and amines is lower than 1 : 1 ($n < m$), the polymer is

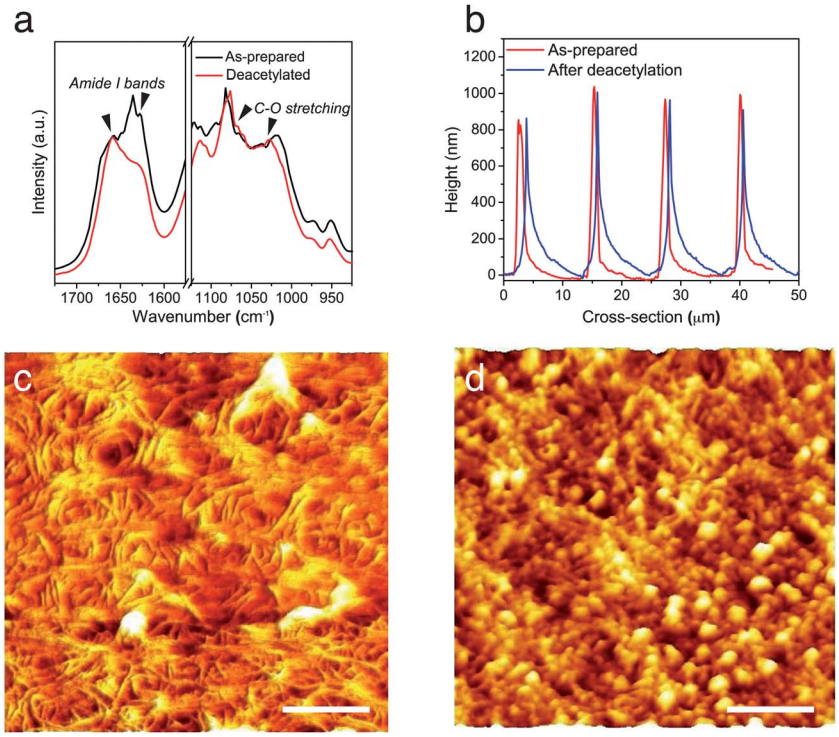

Fig. 3 Effect of the post-treatment of chitin substrates for biological testing (deacetylation in NaOH, fibronectin treatment). (a) FTIR spectra. (b) Cross-sectional height profiles of the chitin substrates obtained from the G2 grating mold. (c and d) Morphology of chitin nanofiber films after deacetylation in NaOH and fibronectin treatment, respectively (all scale bars = 200 nm).

typically referred to as chitosan. This deacetylation process of the chitin nanofibers allowed fine-tuning of the chemistry of the substrates. The degree of deacetylation ($m/(n+m)$) of the chitin nanofiber substrates was determined by FTIR analysis (Fig. 3a) using the ratios of the C–O (amide II) peak at 1560 cm^{-1} and the C–O peak at 1030 cm^{-1}.[28,35] The "as prepared" film was *ca.* 14% deacetylated, while after treatment the degree of deacetylation increased to *ca.* 30%. Importantly, 30% deacetylation did not significantly affect the quality of the micropatterns (Fig. 3b). The deacetylation process to form 30% deacetylated chitin starting from 16% deacetylated chitin was easier than increasing the degree of acetylation of highly deacetylated chitosan as previously reported.[20] Highly deacetylated chitosan does not self-assemble into nanofibers from solution because the nanofiber self-assembly process is driven by the intramolecular hydrogen bonding of the acetyl groups in chitin.[39] However, reducing the number of acetyl groups from 84% to 70% in the self-assembled chitin nanofibers did not disrupt the nanofiber morphology (Fig. 3c) indicating that enough acetyl groups were still present to maintain the hydrogen bonding of the nanofiber structures. Nanofibers with a high surface area provide abundant adhesion sites and enhance the overall cell–substrate interaction. However, further studies with similarly deacetylated chitin without a nanofiber structure are required to pinpoint the exact effects of the nanofiber morphology on cell proliferation, growth, and alignment. Chitin substrates with 30% degree of deacetylation were typically more stable in culture media than the easier to process highly deacetylated chitosan. Highly deacetylated chitosan is soluble in slightly acidic water and often requires additional chemical modification and crosslinking to retain the structural integrity in aqueous environments.[40] Furthermore, coating the samples with FN retained the quality of the micropatterns for cell-culture experiments. While deacetylation did not affect the nanofiber morphology, FN coating was present on top of the nanofibers (Fig. 3c and d). In particular, FN formed globules that were approximately 20 nm in diameter on top of the nanofiber substrates. It is conceivable that these FN globules may assemble along the chitin nanofibers as it is suggested by the topography as seen in Fig. 3d. However, further studies are required to determine the exact FN–chitin interaction and its effects on the FN structure.

To evaluate the use of chitin substrates for tissue engineering, we cultured NIH-3T3 cells on the micropatterned and control chitin substrates and measured cell attachment, alignment, and proliferation. On the chitin micropatterned substrates, G1 and G2 (Fig. 4a and b) cells with a spindle-like morphology aligned their cytoskeletal structure along the major axis of the micropatterned features (contact guidance). In contrast, the cells grown on the control chitin substrates did not have any preferred orientation (Fig. 4c). We further quantified cell nuclei alignment on G1 and G2 micropatterns after 5 days of cell culture (Fig. 4d–f). In G1 and G2, a larger proportion of the cells aligned within the 0–10° preferred angle range as

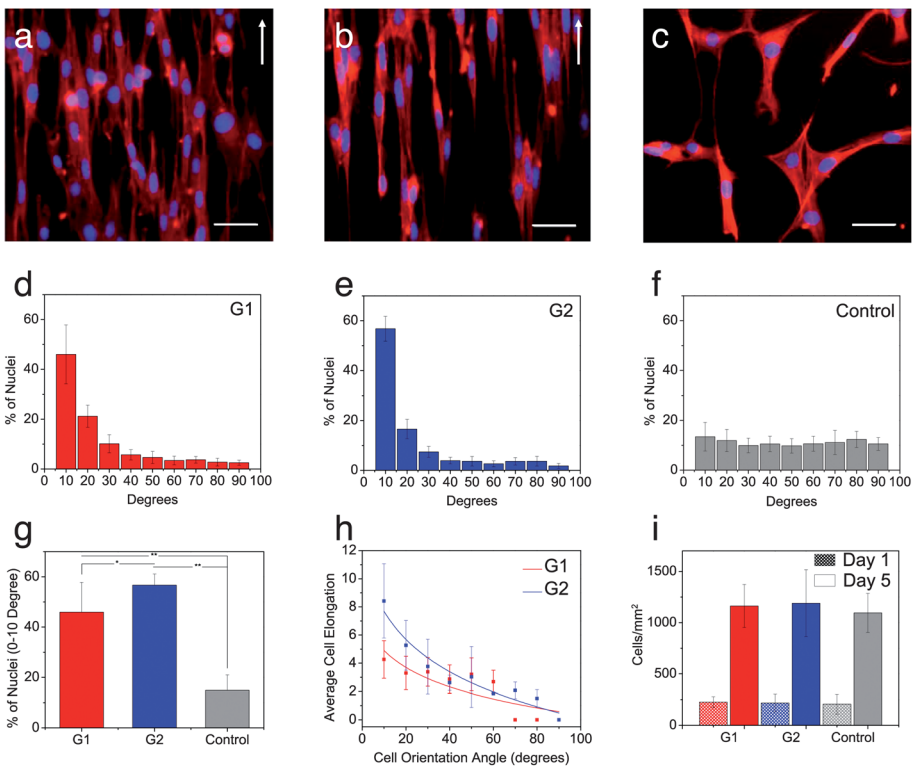

Fig. 4 Fluorescence images of the actin cytoskeleton of the cells on (a) G1, (b) G2 substrates and (c) control sample after 5 days of culture (scale bar 50 μm). The white arrow shows the longitudinal direction of the patterns. (d–f) Distribution of cell nuclei alignment angles on the patterned and control samples. (g) Percentage of cells that have orientation angles within 0–10 degree angles. (h) Cellular elongation function of cell orientation angle within the patterned substrates. (i) Proliferation of the cells on the patterned and control substrates (*P < 0.01 and **P < 0.001).

opposed to the control substrate (Fig. 4f). The degree of cell nuclei alignment on G1 (~45%) and G2 (~55%) samples was significantly higher ($p < 0.05$) than the degree of alignment for the control sample (15%) (Fig. 4g). In addition, on G1 and G2, cell elongation increased with cell alignment. This increase indicated that the substrate topography affected the cell morphology along with cellular alignment (Fig. 4h). Cell attachment and proliferation were also evaluated with the direct cell counting method at days 1 and 5 of culture. NIH-3T3 fibroblast cells proliferated at day 5 of culture compared to day 1, indicating that the chitin substrates were non-cytotoxic. In addition, there was no significant difference in cell proliferation on different micropatterned samples (G1 and G2) compared to the control substrate (Fig. 4i). Our observations are consistent with earlier work in terms of cellular alignment on micropatterns.[41] In general, a decrease in groove width and an increase in groove depth enhance cellular alignment.[41] We observed more pronounced alignment on the G2 micropatterns, which are not only wider, but also deeper than the G1 micropatterns. In G1 micropatterned features, where the cells' size is larger than the groove width and the groove width is decreased beyond a threshold, the cells easily bridge the neighboring ridges. Such behavior ultimately results in an overall decreased cellular alignment. On the other hand, on G2 micropatterns, where the groove width was within the range of a single cell size (10 μm), the cells were laterally confined within the grooves in between the taller ridges. This confinement resulted in improved cellular alignment (ESI, Fig. S1†). Having the groove width in the range of a single cell size, the effect of the width on G2 patterns is expected to be more pronounced on cellular alignment compared to the height. However, some effects on cellular alignment from the increased height in the G2 patterns with respect to G1 cannot be completely ruled out at this stage.

The NIH-3T3-seeded free-standing films were sturdy and easy to manipulate as well as flexible (Fig. 5a) noting that the substrates absorb water and expand up to five fold of their initial volume. Absorption of water is not surprising because the chitin nanofiber substrates themselves are hydrophilic and porous with a density of ~1 g cm^{-3}, which is lower than the density of chitin (1.44 g cm^{-3}). Water absorption and porosity are desirable properties to afford tunable optimal flow of nutrients to, and waste from, the growing tissue.[1] To gather further insights into the mechanical properties of the substrates, we performed a tensile test of the pristine chitin substrates, as well as the 30% deacetylated chitin nanofiber substrates before and after immersion in cell culture media for 1 and 5 days. The elastic modulus (E) of the pristine dry chitin substrates was 2.5 GPa with a tensile strength exceeding 100 MPa (Fig. 5b). As expected from partial removal of the acetyl groups and the corresponding lower degree of hydrogen bonding, the elastic modulus of the chitin substrates after deacetylation to 30% decreased to 926 MPa still retaining a tensile strength of 60 MPa (Fig. 5b). These values for elastic modulus and tensile strength are significantly higher than the values previously reported for chitosan electrospun nanofibers (150 MPa).[42] Even after deacetylation to 30%, the self-assembled chitin nanofibers most likely still have a higher degree of crystallinity and stronger intramolecular hydrogen bonding from the remaining acetyl groups.[39] Notably, only a small decrease in the elastic modulus was observed for the 70% acetylated chitin nanofiber substrates after immersion in DPBS for 1 day (E = 875 MPa) and 5 days (E = 674 MPa) when measured after drying

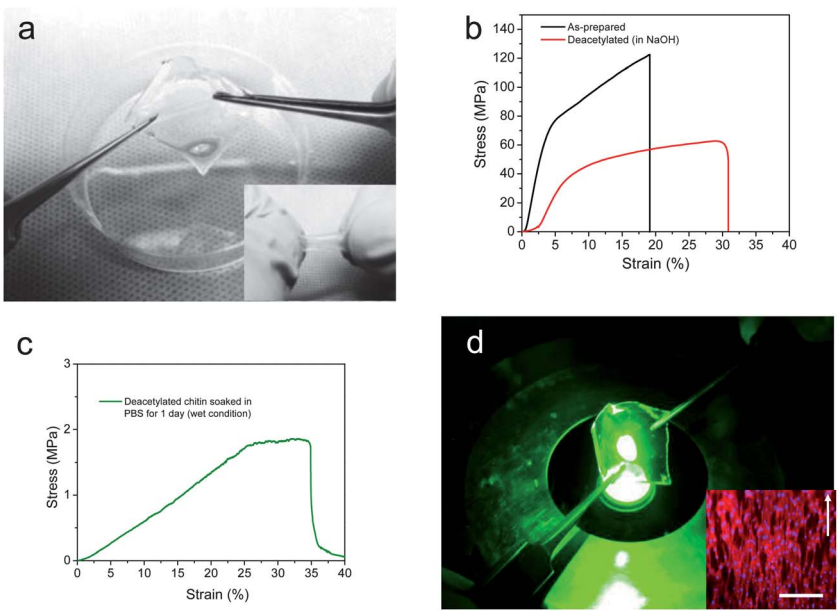

Fig. 5 Cell seeded free-standing flexible chitin substrates. (a) Stretching and rolling (inset) flexibility of the free-standing micropatterned chitin substrates (G2) seeded with 3T3 fibroblasts. (b) Mechanical properties of micropatterned free standing chitin substrates before and after deacetylation to 30%. (c) Mechanical properties of the 30% deacetylated chitin nanofiber substrates after immersion in DPBS for 1 day (measured wet). (d) Chitin nanofiber substrates are transparent and afford optical inspection. (Inset) Fluorescence images of the actin cytoskeleton of the cells on G2 showing the entire coverage and alignment of cells within the direction of the patterned features. The white arrow on the right corner of the inset image indicates the direction of the patterns. Scale bar 100 μm.

off the excess water from the substrates for 30 minutes under ambient conditions (Fig. S2†). These measurements confirmed the stability of the 30% deacetylated chitin nanofiber substrates in cell culture media. The tensile strength of the substrates immersed in DPBS for 1 and 5 days decreased, however, to ~35 MPa. This lower value for tensile strength may be attributed to a higher water content (~25–30%) of the DPBS immersed substrates with respect to the 30% deacetylated dry chitin nanofiber substrates (~10%). However, some degradation of the substrate material cannot be completely ruled out. To investigate the mechanical properties of the substrates during cell culture, we measured substrates after immersion in DPBS for 1 day immediately after removal from the solution while the substrates were still in the swollen state. The elastic modulus was 5 MPa with a tensile strength of 1 MPa (Fig. 5c). Incorporation of water made the substrates more flexible and better suited for tissue engineering applications.[19,43] In these applications it is desirable for the substrate to have similar mechanical properties of the host tissue.[44–46] The substrates formed in this way were transparent, which allows the optical characterization of the cell interaction with the substrate (Fig. 5d). In addition, the cells spread and covered the entire film and aligned along the micropattern major axis as already observed on the glass-supported chitin substrates (Fig. 5d). With these favorable properties, the cell-seeded chitin substrates were still mechanically robust but more flexible than the dry chitin substrates and withstood bending and rolling to produce more complex 3D structures or transfer to the tissue of choice. These transparent, robust, ultra-thin, free-stranding chitin substrates covered with aligned fibroblasts with tunable and superior mechanical properties could make a very promising candidate to form 3D functional tissue and mimic the complex hierarchical structure of the ECM.

Conclusions

In this work, we have developed supported and free-standing micropatterned substrates made of self-assembled chitin nanofibers. These ultrathin micropatterned substrates are biodegradable, mechanically robust, yet flexible and easy to manipulate. The substrates were seeded with NIH-3T3 cells that aligned along the major micropattern axis creating ultra-thin (<10 μm) and free-standing ordered cell sheets. These sheets are sturdy in cell culture media, yet flexible and can be easily manipulated to create more complex tissue structures for regenerative medicine and tissue engineering applications. These applications include myocardial repair where the damaged tissue could be mechanically supported by the chitin substrate while the new tissue is growing. Additionally, these chitin substrates are optically transparent and may find use in retinal regeneration.

Acknowledgements

A. K. acknowledges funding from the Presidential Early Career Award for Scientists and Engineers (PECASE), the Office of Naval Research Young National Investigator Award, the National Science Foundation CAREER Award (DMR 0847287), and the National Institutes of Health (HL092836, AR057837, DE021468, DE019024, EB012597, HL099073, EB008392). M. R. acknowledges funding from the Washington Research Foundation, the University of Washington Center for Commercialization, the Coulter Foundation, and a 3M Untenured Faculty Award.

References

1 A. Khademhosseini, R. Langer, J. Borenstein and J. P. Vacanti, *Proc. Natl. Acad. Sci. U. S. A.*, 2006, **103**, 2480–2487.
2 P. Zorlutuna, N. Annabi, G. Camci-Unal, M. Nikkhah, J. M. Cha, J. W. Nichol, A. Manbachi, H. Bae, S. Chen and A. Khademhosseini, *Adv. Mater.*, 2012, **24**, 1782–1804.
3 T. Dvir, B. P. Timko, D. S. Kohane and R. Langer, *Nat. Nanotechnol.*, 2011, **6**, 13–22.
4 D. E. Discher, P. Janmey and Y. L. Wang, *Science*, 2005, **310**, 1139–1143.
5 S. Kaihara, J. Borenstein, R. Koka, S. Lalan, E. R. Ochoa, M. Ravens, H. Pien, B. Cunningham and J. P. Vacanti, *Tissue Eng.*, 2000, **6**, 105–117.
6 J. T. Borenstein, H. Terai, K. R. King, E. J. Weinberg, M. R. Kaazempur-Mofrad and J. P. Vacanti, *Biomed. Microdevices*, 2002, **4**, 167–175.
7 G. Vozzi, C. Flaim, A. Ahluwalia and S. Bhatia, *Biomaterials*, 2003, **24**, 2533–2540.
8 K. King, C. Wang, M. Kaazempur-Mofrad, J. Vacanti and J. Borenstein, *Adv. Mater.*, 2004, **16**, 2007–2012.
9 C. Fidkowski, M. R. Kaazempur-Mofrad, J. Borenstein, J. P. Vacanti, R. Langer and Y. Wang, *Tissue Eng.*, 2005, **11**, 302–309.
10 C. J. Bettinger, R. Langer and J. T. Borenstein, *Angew. Chem.*, 2009, **48**, 5406–5415.
11 F. Zhao, J. J. Veldhuis, Y. Duan, Y. Yang, N. Christoforou, T. Ma and K. W. Leong, *Mol. Ther.*, 2010, **18**, 1010–1018.
12 M. Yamato, A. Kushida and T. Okano, *Tanpakushitsu Kakusan Koso*, 2000, **45**, 1766–1772.
13 T. Shimizu, M. Yamoto, A. Kikuchi and T. Okano, *Tissue Eng.*, 2001, **7**, 141–151.
14 T. Shimizu, M. Yamato, Y. Isoi, T. Akutsu, T. Setomaru, K. Abe, A. Kikuchi, M. Umezu and T. Okano, *Circ. Res.*, 2002, **90**, E40–E48.
15 Y. Miyahara, N. Nagaya, M. Kataoka, B. Yanagawa, K. Tanaka, H. Hao, K. Ishino, H. Ishida, T. Shimizu, K. Kangawa, S. Sano, T. Okano, S. Kitamura and H. Mori, *Nat. Med.*, 2006, **12**, 459–465.
16 Q. Ke, X. Wang, Q. Gao, Z. Wu, P. Wan, W. Zhan, J. Ge and Z. Wang, *J. Tissue Eng. Regener. Med.*, 2011, **5**, 138–145.
17 Y. Haraguchi, T. Shimizu, M. Yamato and T. Okano, *RSC Adv.*, 2012, **2**, 2184–2190.
18 H. Obokata, M. Yamato, S. Tsuneda and T. Okano, *Nat. Protoc.*, 2011, **6**, 1053–1059.
19 A. W. Feinberg, A. Feigel, S. S. Shevkoplyas, S. Sheehy, G. M. Whitesides and K. K. Parker, *Science*, 2007, **317**, 1366–1370.

20 A. Francesko and T. Tzanov, *Adv. Biochem. Eng./Biotechnol.*, 2011, **125**, 1–27.
21 G. Wang, X. Hu, W. Lin, C. Dong and H. Wu, *In Vitro Cell. Dev. Biol.: Anim.*, 2011, **47**, 234–240.
22 A. Timnak, F. Y. Gharebaghi, R. P. Shariati, S. H. Bahrami, S. Javadian, H. Emami Sh and M. A. Shokrgozar, *J. Mater. Sci.: Mater. Med.*, 2011, **22**, 1555–1567.
23 T. L. Yang, *Int. J. Mol. Sci.*, 2011, **12**, 1936–1963.
24 R. Jayakumar, K. P. Chennazhi, S. Srinivasan, S. V. Nair, T. Furuike and H. Tamura, *Int. J. Mol. Sci.*, 2011, **12**, 1876–1887.
25 C. Ji, N. Annabi, A. Khademhosseini and F. Dehghani, *Acta Biomater.*, 2011, **7**, 1653–1664.
26 S. I. Jeong, M. D. Krebs, C. A. Bonino, J. E. Samorezov, S. A. Khan and E. Alsberg, *Tissue Eng., Part A*, 2011, **17**, 59–70.
27 L. A. Reis, L. L. Chiu, Y. Liang, K. Hyunh, A. Momen and M. Radisic, *Acta Biomater.*, 2012, **8**, 1022–1036.
28 A. Cooper, C. Zhong, Y. Kinoshita, R. S. Morrison, M. Rolandi and M. Zhang, *J. Mater. Chem.*, 2012, **22**, 3105–3109.
29 R. Jayakumar, D. Menon, K. Manzoor, S. V. Nair and H. Tamura, *Carbohydr. Polym.*, 2010, **82**, 227–232.
30 W. Ji, Y. Sun, F. Yang, J. J. van den Beucken, M. Fan, Z. Chen and J. A. Jansen, *Pharm. Res.*, 2011, **28**, 1259–1272.
31 M. R. Ladd, S. J. Lee, J. D. Stitzel, A. Atala and J. J. Yoo, *Biomaterials*, 2011, **32**, 1549–1559.
32 V. Beachley and X. Wen, *Mater. Sci. Eng., C*, 2009, **29**, 663–668.
33 C. Zhong, A. Cooper, A. Kapetanovic, Z. H. Fang, M. Q. Zhang and M. Rolandi, *Soft Matter*, 2010, **6**, 5298–5301.
34 C. Zhong, A. Kapetanovic, Y. Deng and M. Rolandi, *Adv. Mater.*, 2011, **23**, 4776–4781.
35 Y. Shigemasa, H. Matsuura, H. Sashiwa and H. Saimoto, *Int. J. Biol. Macromol.*, 1996, **18**, 237–242.
36 M. Nikkhah, N. Eshak, P. Zorlutuna, N. Annabi, M. Castello, K. Kim, A. Dolatshahi-Pirouz, F. Edalat, H. Bae, Y. Yang and A. Khademhosseini, *Biomaterials*, 2012, **33**, 9009–9018.
37 M. Papadaki, N. Bursac, R. Langer, J. Merok, G. Vunjak-Novakovic and L. E. Freed, *Am. J. Physiol.: Heart Circ. Physiol.*, 2001, **280**, H168–H178.
38 J. R. Couchman, M. R. Austria and A. Woods, *J. Invest. Dermatol.*, 1990, **94**, 7S–14S.
39 K. Zhang, A. Geissler, S. Fischer, E. Brendler and E. Baucker, *J. Phys. Chem. B*, 2012, **116**, 4584–4592.
40 A. Cooper, N. Bhattarai, F. M. Kievit, M. Rossol and M. Q. Zhang, *Phys. Chem. Chem. Phys.*, 2011, **13**, 9969–9972.
41 M. Nikkhah, F. Edalat, S. Manoucheri and A. Khademhosseini, *Biomaterials*, 2012, **33**, 5230–5246.
42 J. D. Schiffman and C. L. Schauer, *Biomacromolecules*, 2007, **8**, 594–601.
43 M. Lovett, K. Lee, A. Edwards and D. L. Kaplan, *Tissue Eng., Part B*, 2009, **15**, 353–370.
44 G. C. Engelmayr, M. Cheng, C. J. Bettinger, J. T. Borenstein, R. Langer and L. E. Freed, *Nat. Mater.*, 2008, **7**, 1003–1010.
45 T. Dvir, B. P. Timko, M. D. Brigham, S. R. Naik, S. S. Karajanagi, O. Levy, H. Jin, K. K. Parker, R. Langer and D. S. Kohane, *Nat. Nanotechnol.*, 2011, **6**, 720–725.
46 N. Annabi, K. Tsang, S. M. Mithieux, M. Nikkhah, A. Ameri, A. Khademhosseini and A. S. Weiss, *Adv. Funct. Mater.*, 2013, DOI: 10.1002/adfm.201300570.

